Nonlinear Noise Theory for Synchronized Oscillators

KLAUS F. SCHÜNEMANN, MEMBER, IEEE, AND KARL BEHM

Abstract—**A nonlinear theory of noise in synchronized oscillators is outlined, thus extending Kurokawa's work [1] from small to arbitrary injection levels. The description is of phenomenological nature: it uses the describing function method of control theory for calculating the carrier waves, and the circuit theory of periodically driven nonlinear systems for an analysis of the noise sidebands. Simple expressions are derived for the various output noises and noise conversion factors in the case when the nonlinear characteristic of the active device can be described by a third-order (van-der-Pol) polynomial.**

I. Introduction

THE THEORY OF NOISE in free-running and synchronized oscillators of the negative resistance type has recently been established [1] and surveyed [2] by Kurokawa, who combined previous work in a convenient form for explaining microwave oscillator noise performance. Since the nonlinear characteristic of the active device (Gunn element, IMPATT diode, etc.) was approximated by a first-order Taylor series expansion around the operating point, every injection signal must be small compared to the free-running amplitude. Due to this restriction, the applicability of the theory is severely limited. Especially the following cases of practical importance are not met:

1) noise and transfer properties of synchronized oscillators for moderate injection levels ("moderate" means that the injected power is −20 dB or less below the output power of the free-running oscillator);
2) noise in tightly to moderately coupled oscillators for mutual synchronization in a power combining network, or in a mounting structure which contains several active elements, or in a phased array system;
3) noise in subharmonically synchronized oscillators;
4) noise in harmonically synchronized oscillators which are of importance as a frequency-divider circuit;
5) noise in multifrequency oscillators.

In cases 3), 4), and 5), Kurokawa's theory even fails for small injection levels, for these synchronization schemes are based upon the nonlinear interaction of the synchronizing and synchronized signals in the active device.

Manuscript received April 30, 1978.

The authors are with the Institut für Hochfrequenztechnik, Technische Universität, Postfach 3329, D-3300 Braunschweig, Germany.

A further restriction of the general noise theory of [1], [2] is the assumption that the open-circuit noise voltage source does not depend on the signal level. To overcome this, Hines [3], Fikart and Goud [4], and Goedbloed and Vlaardingerbroek [5] developed a large-signal noise theory for IMPATT diodes in free-running oscillators, by applying the theory of parametric systems to the solution of the nonlinear Read equation. Thus the system equations have to be solved twice: for the noise-free carrier amplitudes and, subsequently, for the small perturbation signals at the sideband frequencies, which have been assumed to model the noise behavior. The method can, consequently, be extended to cover the case of a synchronized oscillator, which has been done by Goedbloed and Vlaardingerbroek in [6]. Their theory gives a good quantitative description of noise and transfer properties of locked amplifiers with IMPATT diodes. It takes into account both the bias level and the RF-amplitude dependence of the equivalent noise sources as well as the contribution of upconverted bias noise to the output noise spectrum. The theory has been demonstrated to adequately describe synchronization and noise performance of realized IMPATT diode oscillators.

The work to be reported here deals with the same subject as that in [6] but from a different point of view. It is our aim to outline a nonlinear noise theory for synchronized oscillators by directly extending Kurokawa's work to the case of arbitrary injection levels. The description of the active device is thus phenomenological rather than physical: the nonlinearity has been modeled by a third-order (van-der-Pol-type) polynomial, which leads to lucid and tractable calculations. The method is, hence, suited to be applied to more complex systems as, e.g., mutually coupled oscillators and (sub)harmonically synchronized oscillators. In comparison to the noise theory of [6], one can state: our theory is inferior if reliable, quantitative calculations have to be made concerning a realized oscillator with IMPATT diode. It turns out to be superior: 1) as far as lucidity and tractability of the calculations and as physical insight into the phenomena involved are concerned, 2) if complex synchronization schemes shall be investigated, and 3) if the noise performance of a synchronized oscillator with Gunn element shall be analyzed, because a van-der-Pol-type current–voltage characteristic in parallel to a nearly constant electronic capacitance have been shown to adequately model the nonlinear behavior of a Gunn element [7]. Furthermore, the equivalent

0018-9480/79/0500-0452$00.75

open-circuit noise voltage source (or the short-circuit noise current source) may be assumed to be RF-amplitude-independent in this case.

Our first-order nonlinear noise theory, hence, presents a compromise between Kurokawa's work, which arrives at simple analytical expressions for the oscillator output spectrum, and that of Goedbloed and Vlaardingerbroek, which needs time-consuming computations and a complicated matrix formulation. It will be shown that many of the interesting quantities can be derived in an explicit form, although the nonlinear effect of a large injection signal on the oscillator amplitude and phase has been taken into account.

II. Carrier Wave Analysis

The oscillator will be described by a single-tuned circuit as in [1], [6]. It is shown in Fig. 1. N_A is the nonlinear element, and i_i is an injection current source. This equivalent circuit will later be extended to cover the case of a circulator-coupled oscillator. First of all, the noise-free case shall be regarded. For analyzing the "carrier waves" in the equivalent circuit of Fig. 1, the active device must be represented by its nonlinear characteristic, e.g., by its current–voltage characteristic. Then the describing function method of control theory, which has been introduced into the microwave field in [8], is an adequate tool for an analysis, provided that the filtering effect of the linear part of the network is such that the voltage waveform across the active device can be guessed. It may consist of a finite number of sinusoids, of a bias signal, and of Gaussian noise. This condition normally holds in the case of a microwave oscillator. Then the analysis proceeds in the following way: the voltage waveform being known, the current waveform is calculated from the current–voltage characteristic by Fourier analysis. Then the fundamental components of current and voltage are related by the so-called describing function N_A, which means the effective admittance of the nonlinear device. It is amplitude- and, for dynamic nonlinearities, frequency-dependent. With the nonlinear element being replaced by the quasi-linear operator N_A, the circuit of Fig. 1 can be analyzed by standard techniques yielding amplitude and frequency of the oscillation. For further details and generalizations, the reader is referrred to [8].

Although the shape of the nonlinearity is arbitrary, we will model it by a third-order polynomial, because a van-der-Pol-type characteristic is thought to be a consistent extension of Kurokawa's work towards an inclusion of nonlinear effects. The current–voltage characteristic is hence assumed to be

$$i = -a_1 v + a_2 v^2 + a_3 v^3. \tag{1}$$

The voltage waveform across the active device is given by

$$v = v_0 + \hat{v} \cdot \cos(\omega t). \tag{2}$$

Following [9], the various quantities are normalized

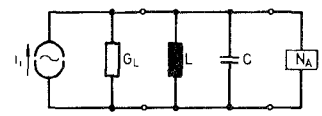

Fig. 1. Simple equivalent circuit of synchronized oscillator.

according to

$$x = v/V_n \qquad y = i/I_n \qquad g_L = G_L/G_n \qquad p = P/P_n$$

with

$$V_n = \sqrt{a_1/a_3} \qquad I_n = a_1 V_n$$
$$G_n = a_1 \qquad P_n = V_n I_n. \tag{3}$$

Equations (1) and (2) can then be rewritten

$$y = -x + ax^2 + x^3 = f(x), \qquad \text{with } a = \sqrt{a_2/(a_1 a_3)} \tag{1a}$$

$$x = x_0 + \hat{x} \cdot \cos(\omega t). \tag{2a}$$

The describing function is defined via

$$n_A = N_A/G_n = \frac{1}{\pi \hat{x}} \int_{-\pi}^{\pi} f(x) \cdot \cos(\omega t) d(\omega t)$$
$$= -1 + 2ax_0 + 3x_0^2 + 3/4\hat{x}^2. \tag{4}$$

Maximizing the power $p_L = P_L/P_n$ in the load conductance with respect to x_0 and g_L yields for the free-running case $y_i = 0$:

$$x_0 = -a/3 \qquad g_L = (1 + a^2/3)/2$$
$$\hat{x}^2 = 2(1 + a^2/3)/3 \qquad p_L = (1 + a^2/3)^2/6. \tag{5}$$

The free-running oscillation frequency is

$$\omega/\omega_0 = 1, \qquad \text{with } \omega_0 = 1/\sqrt{LC}\,. \tag{6}$$

In the case of a nonzero injection current

$$y_i = \hat{y}_i \cdot \cos(\omega_i t + \theta) \tag{7}$$

yields the oscillator node equation

$$[n_A + g_L(1 + j\beta)]\hat{x} = \hat{y}_i \cdot e^{j\theta},$$
$$\text{with } \beta = Q_L(\nu - 1/\nu), \quad \nu = \omega_i/\omega_0, \quad Q_L = \frac{\omega_0 C}{G_L} \tag{8}$$

a third-order polynomial in $\hat{x}^2$, from which the voltage amplitude can be calculated. The phase of the injection current is given by

$$\tan(\theta) = g_L \beta / (3\hat{x}^2/4 + g_L - 1 + 2ax_0 + 3x_0^2). \tag{9}$$

Equations (8) and (9) are valid provided that the oscillator has been locked to the injection signal. In order to investigate the stable synchronization range, the system is tested whether or not additionally injected incremental input signals will grow up or die away with time [8]. It turns out that the effect of the nonlinear element on the incremental signal can be described by a quasi-linear operator n_i which is closely related to n_A via

$$n_i = n_A + \frac{\hat{x}}{2} \frac{\partial n_A}{\partial \hat{x}} (1 + k \cdot e^{-2j\gamma}). \tag{10}$$

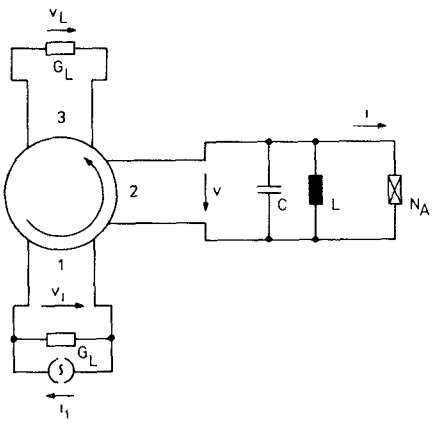

Fig. 2. Equivalent circuit of circulator-coupled locked amplifier.

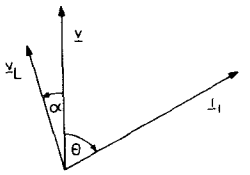

Fig. 3. Phasor diagram for the equivalent circuit of Fig. 2.

In (10) $k=1$ for a synchronous input signal and $k=0$ for a nonsynchronous one. The stability curves of the synchronized oscillator can then be calculated in the following way: The nonlinear element in the equivalent circuit of Fig. 1 is replaced by n_i. Setting $y_i=0$, the oscillator node equation then yields the boundary and locus curves of the oscillator [8]. If the actual voltage amplitude $\hat{x}$ of the synchronized oscillator lies above them, the oscillation is stable; otherwise it is not.

So far, the carrier wave analysis enables us to determine both the voltage amplitude of the oscillation and the stable synchronization range. We will now regard the more realistic equivalent circuit of Fig. 2, in which the injection source and the oscillator are coupled via an ideal circulator. The injected voltage wave $x_i=v_i/V_n$ and the current source y_i are related by

$$x_i=y_i/(2g_L). \tag{11}$$

As the voltage x across the active device is composed of the injected voltage wave x_i plus the reflected voltage wave $x_L=v_L/V_n$, which appears across the load conductance, the latter can be determined from

$$\hat{x}_L\cdot e^{j\alpha}=\hat{x}\cdot e^{j\theta}-\frac{\hat{y}_i}{2g_L}\cdot e^{j\theta}. \tag{12}$$

Here $\hat{x}_L$ means amplitude and α phase of x_L. The corresponding phasor diagram is shown in Fig. 3.

Equations (11) and (12) establish a connection between the equivalent circuits of Figs. 1 and 2. Thus the output power at port 3 of the circulator can be calculated with the injection amplitude $\hat{y}_i$ and the injection frequency ν as parameters.

III. Sideband Noise Analysis

We are in a position now to calculate the AM- and PM-output noise spectra of the synchronized oscillator, which are due to both the intrinsic noise sources and the injected noise from the current source y_i. With respect to the small noise signals, the system is periodically driven by the carriers. Provided that the perturbations are band-limited in a frequency band surrounding the carrier, and that the perturbations are small, the noise analysis should follow the guidelines of a "circuit theory of periodically driven nonlinear systems" which has been formulated by Penfield [10]. It is shown that when the perturbations are expressed in terms of slowly varying voltages and currents, the relations among these voltages and currents are linear and time-invariant. There do exist several ways of representing the perturbations in terms of slowly varying functions of time: the cosine–sine representation, the amplitude–phase representation, and the upper sideband representation have been proposed in [10], while a combination of the lower with the upper sideband has been used in [3]–[6]. The only difference between the well-known network theory for the carriers and that for the sideband signals is that any relation between a perturbation signal at one network port to that at another one is now a matrix equation between the corresponding pairs of sideband signals instead of a simple scalar equation as in the case of the carrier analysis. The elements of such matrices do, of course, depend on the carriers of the nonlinear device.

As the circuit theory for the small perturbation signals is linear, the principle of superposition holds. We will, hence, calculate the contributions to the output noise spectra from the intrinsic and from the injected noise separately.

A. Effect of Intrinsic Noise Sources

The equivalent circuit for the perturbation signals is as shown in Fig. 1. Here the current source i_i may represent the intrinsic short-circuit noise current source of the active device which is composed of a pair of pseudo-sinusoids with random amplitudes and phases at the lower sideband frequency $\omega_l=\omega-\Delta\omega$ and at the upper sideband frequency $\omega_u=\omega+\Delta\omega$. In the following, every voltage or current has to be represented by its lower sideband portion (index "l") and by its upper sideband portion (index "u").

In order to establish a relation between the noise voltage and current at the active device, we assume small perturbations Δy and Δx to be present according to

$$y+\Delta y=f(x+\Delta x),\qquad \Delta y=\frac{df}{dx}\Delta x=f'(x)\Delta x,$$
$$\text{with } f'(x)=-1+2ax+3x^2. \tag{13}$$

$f'(x)$ can be expanded into a Fourier series with coefficients $g_m=G_m/G_n$

$$f'(x)=\sum g_m e^{jm\omega t},$$
$$g_m=\frac{1}{2\pi}\int_{-\pi}^{\pi} f'(x)e^{-jm\omega t}d(\omega t). \tag{14}$$

In the case of a van-der-Pol-type nonlinearity, the g_m are

$$g_0=-1+2ax_0+3x_0^2+3\hat{x}^2/2 \qquad g_1=g_{-1}=a\hat{x}+3x_0\hat{x}$$

$$g_2 = g_{-2} = 3\hat{x}^2/4 \qquad g_m = 0, \qquad \text{for } |m| > 2. \tag{15}$$

If, in addition to the upper and lower sideband vectors, a baseband signal (index "b") at frequency $\Delta\omega$ is assumed too, (13)–(15) yield the desired matrix relation

$$\begin{vmatrix} y_b \\ y_l^* \\ y_u \end{vmatrix} = \begin{vmatrix} g_0 & g_1 & g_1 \\ g_1 & g_0 & g_2 \\ g_1 & g_2 & g_0 \end{vmatrix} \cdot \begin{vmatrix} x_b \\ x_l^* \\ x_u \end{vmatrix}. \tag{16}$$

The asterisk denotes the complex conjugate of the corresponding quantity.

We will in the following restrict ourselves to the case that upconversion from and downconversion to the baseband can be neglected, because this leads to simple analytic expressions for the output noise. Moreover, g_1 turns out to be zero if the bias is adjusted for maximum generated power, as will be shown in the next section. Hence, (16) may be replaced by

$$\begin{vmatrix} y_l^* \\ y_u \end{vmatrix} = \begin{vmatrix} g_0 & g_2 \\ g_2 & g_0 \end{vmatrix} \cdot \begin{vmatrix} x_l^* \\ x_u \end{vmatrix}. \tag{16a}$$

In order to complete the analysis, two node equations have to be added:

$$\begin{aligned} &y_{il} = y_l + x_l g_L(1 + j\beta_l), \\ &y_{iu} = y_u + x_u g_L(1 + j\beta_u), \\ &\beta_l = Q_L(\nu_l - 1/\nu_l), \quad \nu_l = \omega_l/\omega_0 \\ &\beta_u = Q_L(\nu_u - 1/\nu_u), \quad \nu_u = \omega_u/\omega_0. \end{aligned} \tag{17}$$

From (16a) and (17) the noise voltage vectors x_l and x_u can be calculated. Assuming a Gaussian amplitude distribution of the noise current sources y_{il} and y_{iu} according to a spectral density

$$\phi_i = \frac{2\varphi_i^2/\omega_c}{1 + (\omega/\omega_c)^2} \tag{18}$$

with φ_i the variance and ω_c a characteristic frequency, the AM and PM portions of the spectral density of the noise voltage $x_l + x_u$ across the active device are given by

$$\begin{aligned} \phi_{AM} &= \langle \mathrm{Re}^2 (x_l + x_u) \rangle \phi_i \\ \phi_{PM} &= \langle \mathrm{Im}^2 (x_l + x_u) \rangle \phi_i. \end{aligned} \tag{19}$$

The brackets denote an average over the two independent phase angles of y_{il} and y_{iu}. The AM- and PM-noise power spectra follow from (19) according to

$$p_{AM} = \phi_{AM} \cdot g_L \cdot 1 \text{ Hz} \qquad p_{PM} = \phi_{PM} \cdot g_L \cdot 1 \text{ Hz}. \tag{20}$$

It will be shown in the next section that, for some special cases, the evaluation of (19) and (20) leads to simple analytic expressions for the AM- and PM-noise spectra.

In order to calculate the noise power spectra at port 3 of the circulator, the phase shift of the output carrier wave has to be taken into account. According to (12) and the phasor diagram of Fig. 3, the noise voltage $x_l + x_u$ in (19) has to be multiplied by $e^{-j\alpha}$ before the real or imaginary part is taken. With this modification the output noise can be calculated from (19) and (20).

B. Effect of Injected Noise

That part of the output noise spectrum, which is due to the injected noise, is determined by analyzing the equivalent circuit of Fig. 2. The input voltage wave x_i has now to be replaced by a pair x_{il} and x_{iu} of sideband noise vectors. In order to calculate the output noise vectors x_{Ll} and x_{Lu}, the following system of equations has to be solved: 1) the modified node equations

$$\begin{aligned} y_l + x_l g_L(1 + j\beta_l) &= g_L(x_{il} - x_{Ll}) \\ y_u + x_u g_L(1 + j\beta_u) &= g_L(x_{iu} - x_{Lu}) \end{aligned} \tag{21}$$

2) the equations corresponding to (12)

$$x_{Ll} + x_{il} = x_l \qquad x_{Lu} + x_{iu} = x_u \tag{22}$$

and 3) the matrix equation (16a).

It is useful to regard the AM and PM portions of the input noise separately. In the case of injected AM noise the stochastic phase angles are related to one another according to

$$\begin{aligned} x_{il} &= |x_i| e^{-j\epsilon} \cdot e^{j\theta} \\ x_{iu} &= |x_i| e^{j\epsilon} \cdot e^{j\theta} \text{ (AM noise)} \end{aligned} \tag{23}$$

and in the case of PM noise according to

$$\begin{aligned} x_{il} &= -|x_i| e^{-j\epsilon} \cdot e^{j\theta} \\ x_{iu} &= |x_i| e^{j\epsilon} \cdot e^{j\theta} \text{ (PM noise).} \end{aligned} \tag{24}$$

The output noise power spectra due to injected AM or PM noise are then given by

$$\begin{aligned} p_{AM}(\text{AM}) \text{ or } p_{AM}(\text{PM}) &= \langle \mathrm{Re}^2 (x_{Ll} + x_{Lu}) e^{-j\alpha} \rangle \phi_i' \cdot 1 \text{ Hz} \cdot g_L \\ p_{PM}(\text{AM}) \text{ or } p_{PM}(\text{PM}) &= \langle \mathrm{Im}^2 (x_{Ll} + x_{Lu}) e^{-j\alpha} \rangle \phi_i' \cdot 1 \text{ Hz} \cdot g_L \end{aligned} \tag{25}$$

with ϕ_i' the spectral density of the injected noise voltage wave. The average has to be taken over the stochastic phase ϵ.

IV. Discussion of Results

Due to the special choice of the nonlinear characteristic, simple expressions can be derived for the noise spectra in several cases. In order to simplify the evaluation, we will first derive some general relations for the Fourier coefficients g_m.

1) If the bias is adjusted for maximum generated power p_g, g_1 turns out to be zero. This can be proven by regarding

$$p_g = \hat{x}^2 n_A/2 \tag{26}$$

and differentiating with respect to x_0

$$\frac{\partial p_g}{\partial x_0} \sim \frac{\partial n_A(\hat{x}, x_0)}{\partial x_0} = 0. \tag{27}$$

Inserting (4) into (27) yields

$$\frac{\partial n_A}{\partial x_0} = \frac{1}{\pi\hat{x}} \int_{-\pi}^{\pi} f'(x) \frac{dx}{dx_0} \cos(\omega t) d(\omega t). \tag{28}$$

Taking (2a) and (14) into account

$$\frac{\partial n_A}{\partial x_0} = \frac{2}{\hat{x}} g_1 \tag{29}$$

i.e., $g_1 = 0$ for optimum bias.

2) For the free-running oscillator, $g_0 = 0$ is valid. This can be proven by differentiating p_g with respect to x

$$\frac{\partial p_g}{\partial \hat{x}} = \frac{1}{2\pi} \int_{-\pi}^{\pi} f(x) \cos(\omega t)\, d(\omega t) + \frac{\hat{x}}{2\pi} \int_{-\pi}^{\pi} f'(x) \cos^2(\omega t)\, d(\omega t) = \frac{\hat{x}}{2}(n_A + g_0 + g_2). \tag{30}$$

In order to further simplify (30), we integrate the right-hand side of n_A from (4) by parts

$$n_A = \frac{1}{\pi \hat{x}} \left[f(x) \sin(\omega t) \Big|_{-\pi}^{\pi} - \int_{-\pi}^{\pi} f'(x) \frac{dx}{d(\omega t)} \sin(\omega t)\, d(\omega t) \right]. \tag{31}$$

Inserting (2a) yields

$$n_A = g_0 - g_2. \tag{32}$$

This relation holds in general for free-running and for synchronized oscillators.

By combining (30) with (32)

$$\frac{\partial p_g}{\partial \hat{x}} = \hat{x} g_0. \tag{33}$$

Hence, $g_0 = 0$ in the free-running state.

3) Last but not least, the incremental input describing function (10) for a synchronous input signal shall be related to the Fourier coefficients g_m. To this end we write

$$n_i = n_A + \frac{\hat{x}}{2} \frac{dn_A}{d\hat{x}} (1 + \cos(2\gamma) - j \sin(2\gamma)). \tag{34}$$

Using the Fourier integral (4) for n_A, we can verify that

$$\frac{\hat{x}}{2} \frac{dn_A}{d\hat{x}} = g_2. \tag{35}$$

Hence, taking (32) into account,

$$n_i = g_0 + g_2(\cos(2\gamma) - j \sin(2\gamma)). \tag{36}$$

It shall be emphasized that (29), (32), (33), and (36) hold for arbitrary current–voltage characteristics $f(x)$.

Making use of these rather general results, simple expressions can be derived for the AM- and PM-noise spectra. In the case of a free-running oscillator

$$p_{AM} = \phi_i^2 \cdot 1\ \text{Hz} \cdot \frac{1}{2g_L} \frac{1}{1 + \Delta\nu^2 Q_L^2}$$

$$p_{PM} = \phi_i^2 \cdot 1\ \text{Hz} \cdot \frac{1}{2g_L} \frac{1}{\Delta\nu^2 Q_L^2}, \qquad i_i = 0 \tag{37}$$

with $\Delta\nu = \Delta\omega/\omega_0$. Of course, the spectral dependence of both the AM and the PM noise corresponds to what has been derived in [1].

In the case where the oscillator is synchronized at its free-running frequency ($\nu = 1$), the near-carrier output noise ($\Delta\nu \to 0$) due to the intrinsic noise sources is given by

$$p_{AM} = \phi_i^2 \cdot 1\ \text{Hz} \cdot 2g_L \frac{1}{(g_0 + g_2 + g_L)^2}$$

$$p_{PM} = \phi_i^2 \cdot 1\ \text{Hz} \cdot 2g_L \frac{1}{(g_0 - g_2 + g_L)^2},$$

$$\text{for } \nu = 1, \quad \Delta\nu \to 0, \quad i_i \neq 0. \tag{38}$$

The second expression shows the stabilizing effect of the synchronizing signal on the PM noise. For $i_i = 0$ the denominator vanishes because of (32). This gives rise to a sharp PM-noise peak, which is considerably damped even for small injected signals $i_i \neq 0$ for then $n_A \neq g_L$. The AM noise is, on the other hand, only weakly influenced by the injected signal.

Another simple relation, which gives physical insight into the stabilization mechanism, can be obtained for $\nu \neq 1$ but $\Delta\nu \to 0$:

$$p_{AM} = \phi_i^2 \cdot 1\ \text{Hz} \cdot 2g_L \frac{(g_0 - g_2 + g_L)^2 + g_L^2 Q_L^2 (\nu - 1/\nu)^2}{\left((g_0 + g_L)^2 - g_2^2 + g_L^2 Q_L^2 (\nu - 1/\nu)^2\right)^2}$$

$$p_{PM} = \phi_i^2 \cdot 1\ \text{Hz} \cdot 2g_L \frac{(g_0 + g_2 + g_L)^2 + g_L^2 Q_L^2 (\nu - 1/\nu)^2}{\left((g_0 + g_L)^2 - g_2^2 + g_L^2 Q_L^2 (\nu - 1/\nu)^2\right)^2},$$

$$\text{for } \nu \neq 1, \quad \Delta\nu \to 0, \quad i_i \neq 0. \tag{39}$$

It is well known [1] that both AM and PM noise become infinite at the borders of the stable synchronization range. This can be derived from (39) as well if one utilizes (36) in order to calculate the stability condition for synchronous perturbations. It reads

$$n_i + g_L(1 + jQ_L(\nu - 1/\nu)) = 0. \tag{40}$$

Inserting (36) and eliminating γ shows that the left-hand side exactly equals the denominator of (39). The denominator hence coincides with the boundary curve for stable oscillations.

Simple expressions can also be given for the various output noise spectra due to the injected AM or PM noise in the limiting case of $\nu = 1$ and $\Delta\nu \to 0$. Then the AM noise due to AM injection is

$$p_{AM}(\text{AM}) = \phi_i'^2 \cdot 1\ \text{Hz} \cdot 2g_L \frac{\left((g_L - g_2)^2 - g_0^2\right)^2}{\left((g_0 + g_L)^2 - g_2^2\right)^2},$$

$$\text{for } \nu = 1, \quad \Delta\nu \to 0 \tag{41}$$

while $p_{PM}(\text{AM}) = 0$ at $\nu = 1$. The PM noise due to PM injection is

$$p_{PM}(\text{PM}) = \phi_i'^2 \cdot 1\ \text{Hz} \cdot 2g_L \frac{\left((g_L + g_2)^2 - g_0^2\right)^2}{\left((g_0 + g_L)^2 - g_2^2\right)^2},$$

$$\text{for } \nu = 1, \quad \Delta\nu \to 0 \tag{42}$$

while $p_{AM}(\text{PM}) = 0$ at $\nu = 1$.

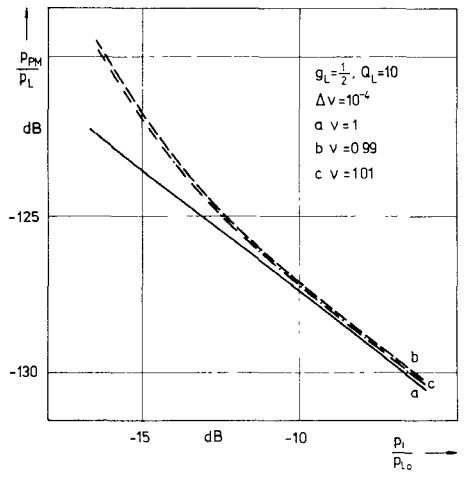

Fig. 4. PM-noise power at the oscillator output due to intrinsic noise versus the injection power (p_L means load power).

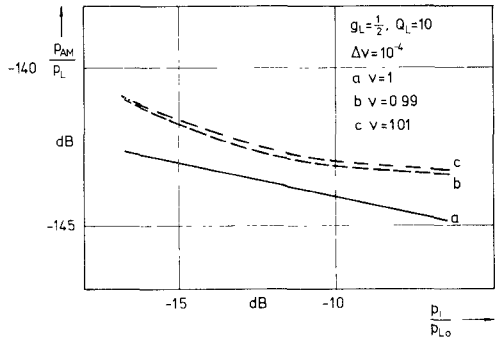

Fig. 5. AM-noise power at the oscillator output due to intrinsic noise versus the injection power (p_L means load power).

Concluding, some numerical examples shall be given. In Fig. 4 (Fig. 5), the intrinsic PM (AM) noise at the circulator output port is shown versus the injected power. The normalizing quantities are given by

$$p_L=\hat{x}_L^2 g_L/2 \qquad p_i=\hat{y}_i^2/(8g_L)$$
$$p_{L0}=p_L(y_i=0)=1/6. \tag{43}$$

ϕ_s has been set to $\phi_s=1/3\times10^{-14}/\text{Hz}$. The frequency stabilization effect increases with increasing injection power. Both AM and PM noise at the circulator output port are typically 1–2 dB larger than at the device port.

The noise conversion factors PMPM, AMAM, and AMPM have been shown versus the injection power in Figs. 6–8. The quantities, which have been labeled by an additional index "0," denote the corresponding values of the free-running oscillator. Supplementary to (43)

$$p_{AM0}=2\phi_i'\cdot 1\ \text{Hz}\cdot g_L\cdot p_{L0}/p_i \tag{44}$$

is the double-sideband AM-noise power of a free-running oscillator which is coupled to port 1 of the circulator via an attenuator with transmission coefficient $p_i/p_{L0}<1$. A similar expression holds for p_{PM0} except that ϕ_i' now is different from ϕ_i' in (44). These spectral densities have been chosen so that $p_{AM0}/p_{L0}=-160$ dB and $p_{PM0}/p_{L0}=-128$ dB.

The PM→PM conversion factor (Fig. 6) is nearly independent from the injection power, while the AM→AM

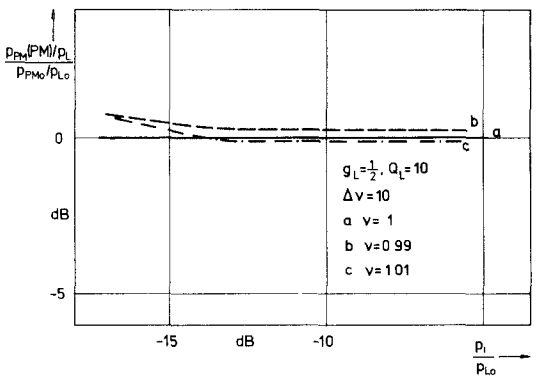

Fig. 6. PM→PM conversion factor of a synchronized oscillator versus the injection power.

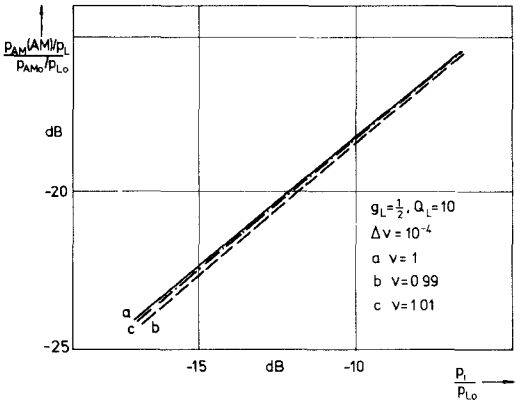

Fig. 7. AM→AM conversion factor of a synchronized oscillator versus the injection power.

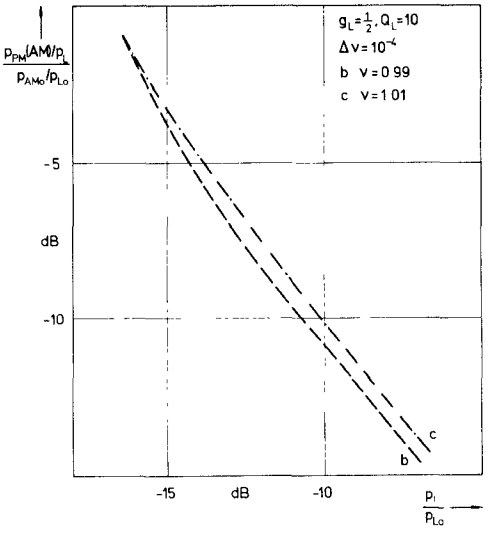

Fig. 8. AM→PM conversion factor of a synchronized oscillator versus the injection power.

conversion factor (Fig. 7) linearly increases with p_i. The AM compression is, however, always better than 10 dB. The AM→PM conversion factor (which is identical to the PM→AM conversion factor) strongly decreases with increasing injection power (Fig. 8). It is, of course, zero for $\nu=1$.

V. Conclusions

A nonlinear theory of noise in synchronized oscillators has been presented which extends Kurokawa's work [1]

from small to arbitrary injection levels. The theoretical approach differs from that of Goedbloed and Vlaardingerbroek [6] in that a phenomenological model of the active device has been chosen which considerably simplifies the mathematical derivations. As a consequence, simple expressions could be obtained for various output noises and noise conversion factors. It is this simplicity that makes the model a suitable means, if more complex synchronization schemes (mutually coupled or (sub) harmonically synchronized oscillators, e.g.) shall be analyzed. Moreover, the model adequately describes the output noise of synchronized oscillators with Gunn elements. It could be extended to account for upconversion and downconversion effects as well as for an RF-amplitude-dependent intrinsic noise source.

References

[1] K. Kurokawa, "Noise in synchronized oscillators," *IEEE Trans. Microwave Theory Tech.*, vol. MTT-16, pp. 234–240, 1968.
[2] ——, "Injection locking of microwave solid-state oscillators," *Proc. IEEE*, vol. 61, pp. 1386–1410, 1973.
[3] M. E. Hines, "Large-signal noise, frequency conversion, and parametric instabilities in IMPATT diode networks," *Proc. IEEE*, vol. 60, pp. 1534–1548, 1972.
[4] J. L. Fikart and P. A. Goud, "A theory of oscillator noise and its application to IMPATT diodes," *J. Appl. Phys.*, vol. 44, pp. 2284–2296, 1973.
[5] J. J. Goedbloed and M. T. Vlaardingerbroek, "Noise in IMPATT diode oscillators at large signal levels," *IEEE Trans. Electron Devices*, vol. ED-21, pp. 342–351, 1974.
[6] ——, "Theory of noise and transfer properties of IMPATT diode amplifiers," *IEEE Trans. Microwave Theory Tech.*, vol. MTT-25, pp. 324–332, 1977.
[7] W. Freude, "Measurement of the statistics of a Gunn oscillator signal and comparison with a mathematical model," *Electron. Commun.*, vol. 30, pp. 209–218, 1976.
[8] L. Gustafsson, G. H. B. Hansson, and K. I. Lundstroem, "On the use of describing functions in the study of nonlinear active microwave circuits," *IEEE Trans. Microwave Theory Tech.*, vol. MTT-20, pp. 402–409, 1972.
[9] M. E. Hines, "Negative-resistance diode power amplification," *IEEE Trans. Electron Devices*, vol. ED-17, pp. 1–8, 1970.
[10] P. Penfield, Jr., "Circuit theory of periodically driven nonlinear systems," *Proc. IEEE*, vol. 54, pp. 266–280, 1966.

Microwave Characterization of Silicon BARITT Diodes Under Large-Signal Conditions

GARY K. MONTRESS, MEMBER, IEEE, AND MADHU SUDAN GUPTA, SENIOR MEMBER, IEEE

***Abstract*—Experimental measurements of the small- and large-signal admittance of a silicon BARITT diode are reported. The structural characteristics of the devices are also reported, so that the results provide a basis for evaluating the large-signal analyses of BARITT diodes. A lumped-element frequency-independent equivalent circuit is proposed to represent the terminal characteristics of the device over a broad-frequency range, and is verified by comparison with the measured admittances. Simple approximations are given to describe the dependence of the device admittance on the three operating point parameters: dc bias current, signal frequency, and RF signal level.**

I. Introduction

OF THE VARIOUS two-terminal, active, microwave semiconductor diodes (e.g., IMPATT, TRAPATT, and Gunn devices), BARITT diodes are known to have the limitations of comparatively small power output, efficiency, bandwidth, and maximum usable frequency, but they also have the advantages of lower noise and simpler technology. One of the principal characteristics of interest is the large-signal admittance Y_D of BARITT diodes, which dictates the design of circuits employing the diodes, as well as determines the power and frequency limitations of the device. This admittance, defined at the terminals of the semiconductor chip (i.e., excluding the effect of parasitics introduced by the diode package), is dependent on three sets of parameters, specifying 1) the semiconductor material properties, 2) the diode doping and dimensions, and 3) the operating conditions, including the dc bias current I_{dc}, the temperature T, the signal frequency f, and RF voltage amplitude V_{RF} of (an assumed) sinusoidal terminal voltage. In this paper, only the functional relationship Y_D (I_{dc}, f, V_{RF}) is studied for a given diode at a given (room) temperature, i.e., with all other parameters fixed.

Large-signal operating characteristics of BARITT diodes have been theoretically studied by a number of authors in the past, both analytically and numerically [1]–[10], and the number of small-signal analyses pub-

Manuscript received May 22, 1978; revised December 1, 1978. This work was supported by the Joint Services Electronics Program.

G. K. Montress was with the Department of Electrical Engineering of the Massachusetts Institute of Technology, Cambridge. He is now with the United Technologies Research Center, East Hartford, CT 06108.

M. S. Gupta is with the Department of Electrical Engineering and Computer Science, and the Research Laboratory of Electronics, Massachusetts Institute of Technology, Cambridge, MA 02139.

0018-9480/79/0500-0458$00.75 ©1979 IEEE